

# Network Coding in Cooperative Communications: Friend or Foe?

Sushant Sharma, *Member, IEEE*, Yi Shi, *Member, IEEE*, Jia Liu, *Member, IEEE*,  
Y. Thomas Hou, *Senior Member, IEEE*, Sastry Kompella, *Member, IEEE*,  
and Scott F. Midkiff, *Senior Member, IEEE*

**Abstract**—A major benefit of employing network coding (NC) in cooperative communications (CC) is its ability to reduce time-slot overhead. Such approach is called network-coded CC (or NC-CC). Most of the existing works have mainly focused on exploiting this benefit without considering its potential adverse effect. In this paper, we show that NC may not always benefit CC. We substantiate this important finding with two important scenarios: employing analog network coding (ANC) in amplify-and-forward (AF) CC, and digital network coding (DNC) in decode-and-forward (DF) CC. For both scenarios, we introduce the important concept of *network coding noise* (NC noise). We analyze the origin of this noise via a careful study of signal aggregation at a relay node and signal extraction at a destination node. We derive a closed-form expression for NC noise at each destination node and show that the existence of NC noise could diminish the advantage of NC in CC. Our results shed new light on how to use NC in CC most effectively.

**Index Terms**—Cooperative communications, network coding, network coding noise.

## 1 INTRODUCTION

**S**PATIAL diversity, in the form of employing multiple antennas (i.e., MIMO), has shown to be very effective in increasing network capacity. However, equipping a wireless node with multiple antennas may not always be practical, as the footprint of multiple antennas may not fit on a wireless node (e.g. a handheld wireless device). In order to achieve spatial diversity without requiring multiple antennas on the same node, the so-called *cooperative communications* (CC) could be employed [15], [16], [21]. Under CC, each node is equipped with only a *single* antenna and spatial diversity is achieved by exploiting the antennas on other (cooperative) nodes in the network.

A simple form of CC can be best illustrated by a three-node example shown in Fig. 1 [16]. In this figure, node  $s$  transmits to node  $d$  via one-hop, and node  $r$  acts as a cooperative relay node. Cooperative transmission from  $s$  to  $d$  is done on a frame-by-frame basis. Within a frame,

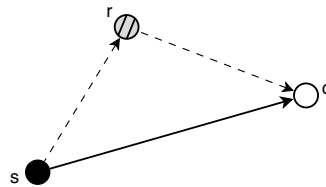


Fig. 1. A three-node schematic for CC.

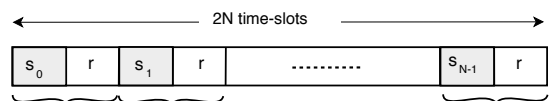


Fig. 2. A frame structure for CC when there are  $N$  source-destination pairs sharing one relay node.

there are two time slots. In the first time slot, source node  $s$  makes a transmission to destination node  $d$ . Due to the broadcast nature of wireless medium, transmission by node  $s$  is also overheard by relay node  $r$ . In the second time slot, node  $r$  forwards the data it overhears in the first time slot to node  $d$ . At destination node  $d$ , the two copies of the data are combined and may improve the data rate between  $s$  and  $d$ .

This three-node example shows CC for a single source-destination session. In general, for multiple sessions sharing the same relay node, it will be necessary to divide a time frame into multiple mini-slots. For example, suppose there are  $N$  source nodes,  $N$  destination nodes, and one relay node. For the  $N$  source-destination pairs to take advantage of CC, one can divide a time frame into  $2N$  mini-slots (see Fig. 2), with every two mini-slots assigned to a session. Note that among the  $2N$  mini-slots, only  $N$  mini-slots are used for transmissions between source and destination nodes. The other  $N$  mini-slots are solely used

- S. Sharma is with Computational Science Center, Brookhaven National Laboratory, Upton, NY, 11973. This work was completed while he was with Virginia Tech, Blacksburg, VA.  
E-mail: sushant@bnl.gov.
- Y. Shi, Y.T. Hou, and S.F. Midkiff are with the Bradley Department of Electrical and Computer Engineering, Virginia Tech, Blacksburg, VA, 24061.  
E-mail: {yshi, thou, midkiff}@vt.edu.
- J. Liu is with the Department of Electrical and Computer Engineering, Ohio State University, Columbus, OH, 43210. This work was completed while he was with Virginia Tech, Blacksburg, VA.  
E-mail: liu@ece.osu.edu.
- S. Kompella is with the Information Technology Division, US Naval Research Laboratory, Washington, DC, 20375.  
E-mail: sastry.kompella@nrl.navy.mil.

Manuscript received 27 May 2010; revised 19 Jan. 2011 and 16 May 2011; accepted 20 May 2011.

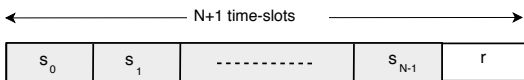


Fig. 3. Time slot structure for CC with NC.

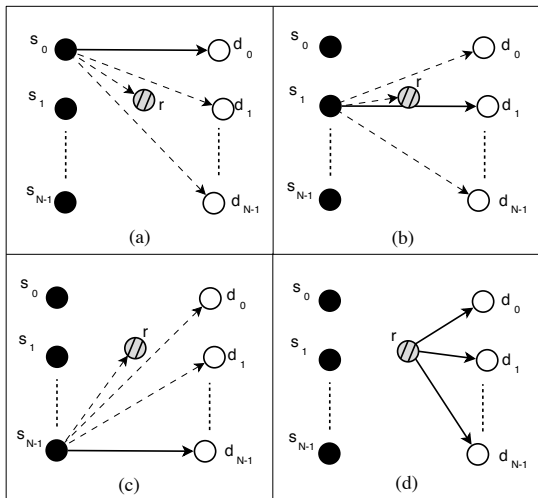


Fig. 4. Sequence of transmissions at  $N$  source nodes and the single relay node.

for transmissions between the relay and destination nodes to complete CC for each of the  $N$  sessions. Obviously, this scheme is wasteful in terms of time slot usage.

A natural question to ask is the following: Is it possible to retain the benefits of CC while reducing its undesirable overhead (in terms of the required number of mini-slots for data relaying)? If this is possible, then the benefits of CC can be extended in a multi-session communication environment.

It turns out that recent advances in *network coding* (NC) [1], [2], [17], [24], [25] offers a key to answer this question. Figure 3 shows a time slot structure of CC with NC. Under this scheme, the source node of each session first transmits in its respective time slot. For a given source node, its transmission is received by the corresponding destination node, and overheard by the cooperative relay node and other destination nodes (see Figs. 4(a)-4(c)). After each source node takes turns to complete its transmission, the relay node performs a linear combination of all the signals that it has overheard in the previous  $N$  time slots. Then the relay node broadcasts the combined signal to all the destination nodes in a *single* time-slot [the  $(N + 1)$ -th time slot in Fig. 3 and Fig. 4(d)]. Then each destination node extracts its desired signal by subtracting the overheard signals from the aggregated signal. We call this approach *network-coded CC* (or NC-CC). In the context of  $N$  source-destination example discussed, NC-CC offers a reduction of  $(N - 1)$  time-slots compared to CC! Further, due to the reduction of the total number of time-slots in a frame, the duration of each time-slot (for transmission) is increased.

Ideally, after the relay node transmits the combined signal, we wish to extract the desired signal at each destination node as cleanly as possible. But as we shall show in

Section 3, a perfect extraction is usually not possible. Just as one would expect, there is no “free lunch” here. In the context of analog network coding (ANC), Section 3.1 shows that there will be a non-negligible noise introduced in the process. Similar situation also occurs in the context of digital network coding (DNC), which we will show in Section 3.2. We call such noise as “network coding noise” (or NC noise), which we find is the main “foe” in NC-CC.

Due to this foe, we find that employing NC in CC may not always be advantageous. To substantiate this finding, we perform an in-depth analysis of NC-CC in the context of (i) ANC [12], [19] with amplify-and-forward (AF) CC [16] (denoted as ANC-CC), and (ii) DNC [11] with decode-and-forward (DF) CC [16] (denoted as DNC-CC). The main results of this paper are as follows.

- We formalize the important concept of NC noise, which we find is the main foe in NC-CC.
- We derive closed form expressions for ANC and DNC noise by studying the signal aggregation process at a relay node and the signal extraction process at a destination node. We also derive mutual information and achievable rate under ANC-CC and DNC-CC.
- Through extensive numerical results, we show the impact of NC noise on NC-CC. Our results offer a new understanding on how to use NC in CC most effectively in light of NC noise.

The remainder of this paper is organized as follows. Section 2 presents related work. In Section 3, we offer an overview of the problems associated with NC-CC in the context of ANC and DNC. In Section 4, we consider ANC-CC and offer a theoretical analysis for the origin of NC noise. We give a mathematical characterization of ANC noise and show how to compute mutual information and achievable rate for each session. In Section 5, we perform a parallel study for DNC-CC. Section 6 presents numerical results and shows the impact of NC noise on NC-CC. Section 7 concludes this paper.

## 2 RELATED WORK

In this section, we briefly review related work in CC and NC. We also review several recent efforts on NC-CC.

The concept of CC can be traced back to the three-terminal communication channel (or a relay channel) in [23] by Van Der Meulen. Shortly after, Cover and El Gamal studied the general relay channel and established an achievable lower bound for data transmission [4]. These two seminal works laid the foundation for the present-day research on CC. Recent research on CC aims to exploit distributed antennas on neighboring nodes in the network, and has resulted in a number of protocols at the physical layer [5], [6], [7], [9], [16], [18], [21], [22] and the network layer [13], [20], [27]. The AF CC and DF CC models used in our study in this paper are based on [16].

The concept of NC was first introduced by Ahlswede *et al.* in their seminal work [1], where they showed how NC can save bandwidth for multicast flows in a wired network. In the context of wireless networks, the most

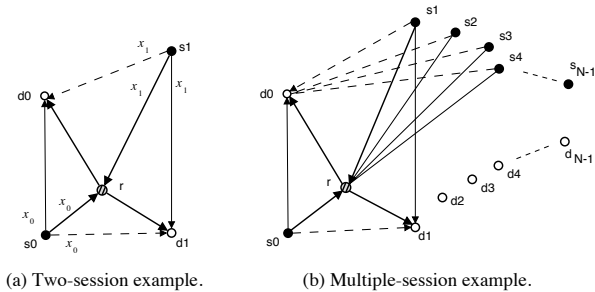


Fig. 5. Examples illustrating NC in CC.

widely studied types of NC are DNC (see e.g. [11]) and ANC (see e.g. [12]). For the state-of-the-art in NC, we refer readers to the NC bibliography in [8].

Recent efforts on NC-CC that are most relevant to our work include [2], [17], [24], [25]. Bao *et al.* [2] were the first to employ NC in CC in a multi-source single-destination network. They showed that NC-CC can improve the achievable rate and outage probability of a network. Shortly after, Peng *et al.* [17] considered a network with a single relay node and multiple source-destination pairs. They again showed that NC can help CC reduce the outage probability of the entire network. More recently, Xiao *et al.* [24] considered a two-source single-destination network and showed that NC can help CC reduce packet error rates. In [25], Xu and Li considered a cellular network with bi-directional traffic, and showed that the network throughput can be increased when NC is employed in CC. These results all show the benefits of applying NC to CC. However, the potential “foe” in NC-CC has not been recognized and explored in these prior efforts.

### 3 THE PROBLEM

In this section, we explore the potential foe in NC-CC in terms of NC noise. To start, we consider an example shown in Fig. 5(a), where there are two source-destination pairs ( $s_0-d_0$  and  $s_1-d_1$ ) and one-relay node ( $r$ ). Both source-destination pairs will use the same relay node for CC and NC is employed at the relay node.

#### 3.1 Analog NC-CC

Based on our discussion for Fig. 3, a frame is divided into three time-slots. In the first time-slot,  $s_0$  broadcasts signal  $x_0$  to  $d_0$ , which is overheard by  $r$  and  $d_1$ ; in the second time slot,  $s_1$  broadcasts signal  $x_1$  to  $d_1$ , which is overheard by  $r$  and  $d_0$ ; then the relay node  $r$  performs ANC by combining the overheard signals from  $s_0$  and  $s_1$ , and then amplifies and broadcasts the combined signal in the third time slot to  $d_0$  and  $d_1$ . The destination node  $d_0$  receives one copy of signal  $x_0$  in the first time slot. It also overhears a copy of signal  $x_1$  (denoted as  $y_{s_1 d_0}$ ) in the second time slot. In the third time slot, destination node  $d_0$  receives the combined signal, denoted as  $y_{s_0 r d_0} + y_{s_1 r d_0}$ .

One would hope that the destination node  $d_0$  in Fig. 5(a) can cleanly extract  $y_{s_0 r d_0}$  by having the combined signal ( $y_{s_0 r d_0} + y_{s_1 r d_0}$ ) subtract the overheard signal  $y_{s_1 d_0}$ . But

in reality,  $y_{s_1 r d_0} \neq y_{s_1 d_0}$  due to two different paths. As a result of such subtraction, a new noise term, called “ANC noise” (for the analog version), will be introduced at  $d_0$ . This noise term is  $[y_{s_1 r d_0} - y_{s_1 d_0}]$ . When the number of sessions increases [see Fig. 5(b)], the sum of noise will increase, and the aggregate noise at  $d_0$  in Fig. 5(b) becomes  $\sum_{i=1}^{N-1} [y_{s_i r d_0} - y_{s_i d_0}]$ . That is, the amount of ANC noise grows as  $N$  increases. Clearly, the benefits of employing ANC will be diminished as ANC noise increases. For a given session, the mutual information (or achievable rate) is a good measure of the benefits of ANC-CC. We will show that the effective mutual information will decrease due to ANC noise.

#### 3.2 Digital NC-CC

In the digital version, the signal combining procedure changes slightly at the relay node when it employs DNC for DF CC. For the two-session example in Fig. 5(a), source node  $s_0$  transmits a signal in the first time slot. This signal is received and *decoded* by the relay node; and overheard by the other destination node  $d_1$ . Similarly, in the second time slot, source node  $s_1$  transmits and the signal is received and decoded by  $r$ ; and overheard by  $d_0$ . In the third time slot, the relay node combines the two decoded signals using DNC, and then transmits the combined signal. To extract the signal, the destination node  $d_0$  subtracts the overheard signal (from  $s_1$  in the second time slot) from the combined signal to obtain the desired signal. Again, due to different paths taken by the signals, the subtraction will result in a noise term, which we call DNC noise. It is easy to see that as the number of sessions on the relay node increase [as in Fig. 5(b)], the DNC noise will also increase. Similar to ANC-CC, the benefits of employing DNC will diminish as DNC noise increases, and so will the effective mutual information.

In the following two sections, we quantify the above discussion through a careful analysis of NC noise, both for analog and digital case. Table 1 shows all notation in this paper.

### 4 THE CASE OF ANC-CC

In this section, we focus on analog version of NC-CC. In Section 4.1, we analyze the ANC noise for ANC-CC. Then in Section 4.2, we derive the achievable rate under ANC-CC in light of ANC noise.

#### 4.1 Analysis of ANC Noise

We first consider the simple two-session example in Fig. 5(a). For this simple network, we analyze the ANC process at the relay node. Then we analyze the signal extraction process of a destination node. This is followed by the derivation of ANC noise. Based on the results for the two-session case, we generalize the results for the  $N$ -session case shown in Fig. 5(b).

TABLE 1  
Notation

Symbol	Definition
$C_{\text{ANC-CC}}(s_i, r_j, d_i)$	Achievable rate for $s_i$ - $d_i$ pair with relay $r_j$ under ANC-CC
$C_{\text{DNC-CC}}^{\text{UB}}(s_i, r_j, d_i)$	Upper bound on the achievable rate for $s_i$ - $d_i$ pair with relay $r_j$ under DNC-CC
$C_{\text{DNC-CC}}^{\text{LB}}(s_i, r_j, d_i)$	Lower bound on the achievable rate for $s_i$ - $d_i$ pair with relay $r_j$ under DNC-CC
$C_{\text{AF}}(s_i, r_j, d_i)$	Achievable rate for $s_i$ - $d_i$ pair with relay $r_j$ under AF CC (no NC)
$C_{\text{DF}}(s_i, r_j, d_i)$	Achievable rate for $s_i$ - $d_i$ pair with relay $r_j$ under DF CC (no NC)
$C_{\text{D}}(s_i, d_i)$	Achievable rate for $s_i$ - $d_i$ pair under direct transmission
$h_{uv}$	A parameter to capture the effect of path loss, shadowing and fading between nodes $u$ and $v$
$N$	Number of source nodes in the network
$r$	Relay node
$x_s$	Signal transmitted by node $s$
$y_{uv}$	Received signal at node $v$ (from node $u$ )
$y_{(s_i \cup s_j)r d}$	Combination of analog signals from $s_i$ and $s_j$ received by destination node $d$ (with NC at relay node $r$ )
$z_v$	Background noise at node $v$
$z_v^{\text{ANC}}$	ANC noise at node $v$
$z_v^{\text{DNC}}$	DNC noise at node $v$
$s_i$	The $i$ -th source node
$S_r$	Set of source nodes using relay node $r$ to perform ANC-CC
$\text{SNR}_{uv}$	The signal noise ratio at node $v$ when $u$ is transmitting
$W$	Total bandwidth available in the network
$P_u$	Transmission power at node $u$
$\sigma_v^2$	Variance of background noise at node $v$
$\sigma_v^{\text{ANC}}$	Variance of ANC noise at node $v$
$\sigma_v^{\text{DNC}}$	Variance of DNC noise at node $v$
$\alpha_r$	Amplifying factor at relay $r$ for ANC-CC

#### 4.1.1 Two-Session Case

In Fig. 5(a), we assume that the signal  $x_0$  transmitted by source  $s_0$  in the first time slot is for packet  $p_0$ , and the signal  $x_1$  transmitted by source  $s_1$  in the second time slot is for packet  $p_1$ . We use  $h_{s_0 d_0}$  to capture the effect of path-loss, shadowing, and fading between nodes  $s_0$  and  $d_0$ . Assume that the background noise at a node  $r$ , denoted by  $z_r$ , is white Gaussian with zero mean and variance  $\sigma_r^2$ . Denote  $y_{srd}$  as the signal received by a destination node  $d$  that is transmitted by a relay node  $r$  and originated from some source  $s$ . Denote  $y_{sr}$  as the signal received by the relay node  $r$  that is transmitted and originated at some source  $s$ . Denote  $\alpha_r$  as the amplifying factor used by the relay node  $r$ .

**Combining Signals at Relay Node** Since node  $s_0$  transmits in the first time slot, we can express the signals received by  $r$ ,  $d_0$  and  $d_1$  during the first time slot as

$$y_{s_0 r} = h_{s_0 r} x_0 + z_r, \quad (1)$$

$$y_{s_0 d_0} = h_{s_0 d_0} x_0 + z_{d_0},$$

$$y_{s_0 d_1} = h_{s_0 d_1} x_0 + z_{d_1}. \quad (2)$$

In the second time slot, when node  $s_1$  transmits, the

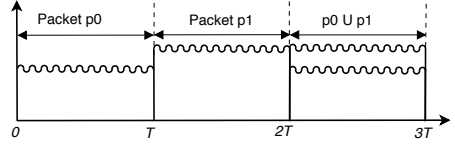


Fig. 6. Transmission behavior of ANC-CC for two sessions.

signals received by  $r$ ,  $d_0$  and  $d_1$  can be expressed as

$$y_{s_1 r} = h_{s_1 r} x_1 + z_r, \quad (3)$$

$$y_{s_1 d_0} = h_{s_1 d_0} x_1 + z_{d_0},$$

$$y_{s_1 d_1} = h_{s_1 d_1} x_1 + z_{d_1}.$$

Then in the third time slot, relay node  $r$  combines  $x_0$  and  $x_1$ , and amplifies and broadcasts the combined signal. Figure 6 shows the transmission behavior of ANC-CC for two sessions.

**Signal Extraction at a Destination Node** To understand how a destination node will separate this combined signal, we focus on one of the destination nodes,  $d_1$ . At  $d_1$ , it has received a combined signal ( $x_0 \cup x_1$ ) from the relay node in the third time slot. It has also overheard signal  $x_0$  transmitted by source  $s_0$  in the first time slot. Using these two signals,  $d_1$  can extract a copy of signal  $x_1$  from the combined signal as follows.

Denote the combined signal received by destination node  $d_1$  in the third time slot as

$$y_{(s_0 \cup s_1) r d_1}(t) = \alpha_r h_{r d_1} [y_{s_0 r}(t - 2T) + y_{s_1 r}(t - T)] + z_{d_1}(t), \quad \forall t \in (2T, 3T], \quad (4)$$

where  $T$  is the length of each time-slot in the frame, and the value of  $\alpha_r$  is chosen as [16]:

$$\alpha_r^2 = \frac{P_r}{|h_{s_0 r}|^2 P_{s_0} + |h_{s_1 r}|^2 P_{s_1} + 2\sigma_r^2}, \quad (5)$$

where  $P_r$ ,  $P_{s_0}$ , and  $P_{s_1}$  are the transmission powers of nodes  $r$ ,  $s_0$ , and  $s_1$ , respectively.

By using (1), the combined signal in (4) can be expanded as

$$y_{(s_0 \cup s_1) r d_1}(t) = \alpha_r h_{r d_1} [h_{s_0 r} x_0(t - 2T) + z_r(t - 2T) + y_{s_1 r}(t - T)] + z_{d_1}(t), \quad \forall t \in (2T, 3T]. \quad (6)$$

Using (2), (6) can be re-written as

$$y_{(s_0 \cup s_1) r d_1}(t) = \frac{\alpha_r h_{r d_1} h_{s_0 r}}{h_{s_0 d_1}} [y_{s_0 d_1}(t - 2T) - z_{d_1}(t - 2T)] + \alpha_r h_{r d_1} y_{s_1 r}(t - T) + z_{d_1}(t) + \alpha_r h_{r d_1} z_r(t - 2T), \quad \forall t \in (2T, 3T]. \quad (7)$$

Equation (7) represents the signal that the destination node  $d_1$  will receive in the third time slot. In the first time slot, destination node  $d_1$  overheard the transmission of  $s_0$ , which is given by (2) and can be re-written as

$$y_{s_0 d_1}(t) = h_{s_0 d_1} x_0(t) + z_{d_1}(t), \quad \forall t \in [0, T]. \quad (8)$$

Since we assume that the channel gains and amplification factor are given, destination node  $d_1$  can multiply (8), by

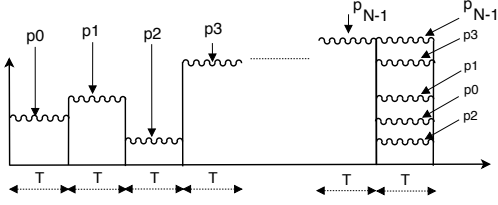


Fig. 7. Transmission behavior of ANC-CC for  $N$  sessions.

a factor  $\frac{\alpha_r h_{rd_1} h_{s_0 r}}{h_{s_0 d_1}}$ , and subtract it from (7). We have

$$\begin{aligned} \hat{y}_{rd_1}(t) &= y_{(s_0 \cup s_1)r d_1}(t) - \frac{\alpha_r h_{rd_1} h_{s_0 r}}{h_{s_0 d_1}} y_{s_0 d_1}(t - 2T) \\ &= \alpha_r h_{rd_1} y_{s_1 r}(t - T) + z_{d_1}(t) + \alpha_r h_{rd_1} z_r(t - 2T) \\ &\quad - \frac{\alpha_r h_{rd_1} h_{s_0 r}}{h_{s_0 d_1}} z_{d_1}(t - 2T), \quad \forall t \in (2T, 3T] \end{aligned} \quad (9)$$

Equation (9) represents the signal for packet  $p_1$  that destination node  $d_1$  can construct, using the combined signal received in the third time slot and the signal overheard in the first time slot. We find that instead of  $z_{d_1}$ , we now have a new noise term in this constructed signal, which we denote as  $z_{d_1}^{\text{ANC}}$ , i.e.,

$$\begin{aligned} z_{d_1}^{\text{ANC}}(t) &= z_{d_1}(t) + \alpha_r h_{rd_1} z_r(t - 2T) - \\ &\quad \frac{\alpha_r h_{rd_1} h_{s_0 r}}{h_{s_0 d_1}} z_{d_1}(t - 2T), \quad \forall t \in (2T, 3T]. \end{aligned} \quad (10)$$

We call  $z_{d_1}^{\text{ANC}}$  ‘‘ANC noise’’. Note that  $z_{d_1}^{\text{ANC}}$  has a zero mean (because  $E[z_{d_1}] = E[z_r] = 0$ ) and its variance is

$$\sigma_{z_{d_1}^{\text{ANC}}}^2 = \sigma_{d_1}^2 + (\alpha_r h_{rd_1})^2 \sigma_r^2 + \left( \frac{\alpha_r h_{s_0 r} h_{rd_1}}{h_{s_0 d_1}} \right)^2 \sigma_{d_1}^2, \quad (11)$$

which is larger than the original noise variance  $\sigma_{d_1}^2$ .

#### 4.1.2 The $N$ -Session Case

We now consider the general case, where there are  $N$  source-destination pairs and one relay node in the network [see Fig. 5(b)]. To have all  $N$  source-destination pairs share the same relay node with ANC,  $(N + 1)$  time slots are needed (see Fig. 3). The signal aggregation process in this scenario follows the same token as in the two-session case. Figure 7 shows the details in each time slot.

In this  $N$ -session case, a given destination node  $d_i$  overhears a copy of all the packets (including  $p_i$ ) during the first  $N$  time slots. In order to construct the signal for the second copy of packet  $p_i$ , the destination node  $d_i$  will again follow the same procedure as in the two-session case. Now, instead of subtracting only one signal from the combined signal, the destination node will need to subtract the signals overheard from  $(N - 1)$  sources. The expressions for the ANC noise can be obtained by generalizing (10) as follows

$$\begin{aligned} z_{d_i}^{\text{ANC}}(t) &= z_{d_i}(t) + \sum_{s_j \in \mathcal{S}_r, s_j \neq s_i} \alpha_r h_{rd_i} z_r(t - |\mathcal{S}_r|T) - \\ &\quad \sum_{s_j \in \mathcal{S}_r} \frac{\alpha_r h_{rd_i} h_{s_j r}}{h_{s_j d_i}} z_{d_i}(t - |\mathcal{S}_r|T), \\ &\quad \forall t \in (|\mathcal{S}_r|T, (|\mathcal{S}_r| + 1)T), \end{aligned} \quad (12)$$

where  $\mathcal{S}_r$  is the set of  $N$  source nodes that are using relay  $r$ , and a general expression for the amplification factor  $\alpha_r$

can be obtained by generalizing (5), which is

$$\alpha_r^2 = \frac{P_r}{|\mathcal{S}_r| \sigma_r^2 + \sum_{s_i \in \mathcal{S}_r} P_{s_i} |h_{s_i r}|^2}. \quad (13)$$

The variance of ANC noise can be obtained by generalizing (11), which is

$$\begin{aligned} \sigma_{z_{d_i}^{\text{ANC}}}^2 &= \sigma_{d_i}^2 + (|\mathcal{S}_r| - 1) (\alpha_r h_{rd_i})^2 \sigma_r^2 + \\ &\quad \sigma_{d_i}^2 \sum_{s_j \in \mathcal{S}_r, s_j \neq s_i} \left( \frac{\alpha_r h_{s_j r} h_{rd_i}}{h_{s_j d_i}} \right)^2. \end{aligned} \quad (14)$$

We see that the variance of ANC noise at destination node  $d_i$  contains  $\sigma_{d_i}^2$  and some additional new terms. These additional new terms are introduced due to the relay node employing ANC for aggregating multiple signals from sources in  $\mathcal{S}_r$ . The variance of ANC noise at the destination nodes increases with the number of sessions sharing the same relay node.

## 4.2 Computing Achievable Rate

### 4.2.1 ANC-CC

To compute the achievable rate under ANC-CC, we denote the time duration of the entire frame as  $t$  seconds. As a result, when all  $N$  sessions are sharing the same relay node with ANC-CC (see Fig. 3), every source node and the relay node will get a time-slot of  $T = \frac{t}{N+1}$  seconds. Then the achievable rate for a session, say  $(s_i, d_i)$ , is

$$\begin{aligned} C_{\text{ANC-CC}}(s_i, r, d_i) &= \left( \frac{\frac{t}{N+1}}{t} \right) \cdot W I_{\text{ANC-CC}}(s_i, r, d_i) \\ &= \frac{W}{N+1} \cdot I_{\text{ANC-CC}}(s_i, r, d_i), \end{aligned} \quad (15)$$

where  $I_{\text{ANC-CC}}(s_i, r, d_i)$  is the mutual information between  $s_i$  and  $d_i$ , and  $W$  is the available bandwidth in the network. In (15), the effective bandwidth for session  $(s_i, d_i)$  is  $W$  divided by  $(N + 1)$  ( $N$  source nodes plus one relay) in the network.

To derive the mutual information  $I_{\text{ANC-CC}}(s_i, r, d_i)$  between session  $(s_i, d_i)$ , we need to consider the ANC noise [Eq. (14)] at the destination nodes. For the signal transmitted by a source node  $s_i$ , the received signal at the relay node is

$$y_{s_i r} = h_{s_i r} x_i + z_r, \quad (16)$$

and the received signal at the corresponding destination node is

$$y_{s_i d_i} = h_{s_i d_i} x_i + z_{d_i}. \quad (17)$$

For the signal transmitted by the relay node, the desired signal at the destination node (after extraction) is

$$\hat{y}_{rd_i} = \alpha_r h_{rd_i} y_{s_i r} + z_{d_i}^{\text{ANC}},$$

which is

$$\hat{y}_{rd_i} = \alpha_r h_{rd_i} (h_{s_i r} x_i + z_r) + z_{d_i}^{\text{ANC}}, \quad (18)$$

where  $z_{d_i}^{\text{ANC}}$  is given in (12) and  $\alpha_r$  is given in (13).

We can re-write (16), (17) and (18) into the following compact matrix form

$$\mathbf{Y} = \mathbf{H}x_i + \mathbf{BZ},$$

where

$$\mathbf{Y} = \begin{bmatrix} y_{s_i d_i} \\ \hat{y}_{r d_i} \end{bmatrix}, \quad \mathbf{H} = \begin{bmatrix} h_{s_i d_i} \\ h_{r d_i} \alpha_r h_{s_i r} \end{bmatrix},$$

$$\mathbf{B} = \begin{bmatrix} 0 & 1 & 0 \\ \alpha_r h_{r d_i} & 0 & 1 \end{bmatrix}, \quad \text{and} \quad \mathbf{Z} = \begin{bmatrix} z_r \\ z_{d_i} \\ z_{d_i}^{\text{ANC}} \end{bmatrix}.$$

It was shown in [16] that we can model the above channel that combines both the direct path ( $s_i$  to  $d_i$ ) and the relay path ( $s_i$  to  $r$  to  $d_i$ ) as a one-input two-output complex Gaussian vector channel. The mutual information between  $s_i$  and  $d_i$  is

$$I_{\text{ANC-CC}}(s_i, r, d_i) = \log_2 \det \left( \mathbf{I} + (P_{s_i} \mathbf{H} \mathbf{H}^\dagger) (\mathbf{B} \mathbf{E} [\mathbf{Z} \mathbf{Z}^\dagger] \mathbf{B}^\dagger)^{-1} \right), \quad (19)$$

where  $\mathbf{I}$  is the identity matrix,  $\dagger$  represents the complex conjugate transpose,  $E[\cdot]$  is the expectation function, and

$$E[\mathbf{Z} \mathbf{Z}^\dagger] = \begin{bmatrix} \sigma_r^2 & 0 & 0 \\ 0 & \sigma_{d_i}^2 & 0 \\ 0 & 0 & \sigma_{z_{d_i}^{\text{ANC}}}^2 \end{bmatrix}.$$

Expanding (19) gives us the mutual information

$$I_{\text{ANC-CC}}(s_i, r, d_i) = \log_2 \left( 1 + \frac{|h_{s_i d_i}|^2 P_{s_i}}{\sigma_{d_i}^2} + \frac{P_{s_i} |h_{r d_i} \alpha_r h_{s_i r}|^2}{|h_{r d_i} \alpha_r|^2 \sigma_r^2 + \sigma_{z_{d_i}^{\text{ANC}}}^2} \right),$$

which can be further rewritten as

$$I_{\text{ANC-CC}}(s_i, r, d_i) = \log_2 \left( 1 + \text{SNR}_{s_i d_i} + \frac{\text{SNR}_{s_i r} \text{SNR}_{r d_i}}{|\mathcal{S}_r| \frac{\sigma_{z_{d_i}^{\text{ANC}}}^2}{\sigma_{d_i}^2} + \text{SNR}_{r d_i} + \frac{\sigma_{z_{d_i}^{\text{ANC}}}^2}{\sigma_{d_i}^2} \sum_{s_j \in \mathcal{S}_r} \text{SNR}_{s_j r}} \right), \quad (20)$$

where  $\text{SNR}_{s_i d_i} = \frac{P_{s_i}}{\sigma_{d_i}^2} |h_{s_i d_i}|^2$ ,  $\text{SNR}_{s_i r} = \frac{P_{s_i}}{\sigma_r^2} |h_{s_i r}|^2$ , and  $\text{SNR}_{r d_i} = \frac{P_r}{\sigma_{d_i}^2} |h_{r d_i}|^2$ .

For the special case of  $|\mathcal{S}_r| = 1$ , i.e., for one-session (three-node model), we have  $i = 0$ ,  $\sigma_{z_{d_i}^{\text{ANC}}}^2 = \sigma_{d_i}^2$ , and (20) is reduced to

$$I_{\text{AF}}(s_i, r, d_i) = \log_2 \left( 1 + \text{SNR}_{s_i d_i} + \frac{\text{SNR}_{s_i r} \text{SNR}_{r d_i}}{1 + \text{SNR}_{r d_i} + \text{SNR}_{s_i r}} \right), \quad (21)$$

which is exactly the result for the simple three-node model in [16].

For a given session, it is worth comparing its achievable rate under ANC-CC [in (15)] with the achievable rates when (i) the session performs AF CC without ANC, and (ii) the session employs direct transmission. We now give the achievable rates of the latter two schemes for comparison.

#### 4.2.2 AF CC (without ANC)

Under this scheme [16], the session performs AF CC, but the relay node does not employ ANC. Each source node and the relay node will get a time-slot of  $t/2N$  (see Fig. 2). Using (21), the achievable rate for a session ( $s_i, d_i$ ) is

$$C_{\text{AF}}(s_i, r, d_i) = \left( \frac{t}{2N} \right) W I_{\text{AF}}(s_i, r, d_i) = \frac{W}{2N} \log_2 \left( 1 + \text{SNR}_{s_i d_i} + \frac{\text{SNR}_{s_i r} \text{SNR}_{r d_i}}{1 + \text{SNR}_{r d_i} + \text{SNR}_{s_i r}} \right). \quad (22)$$

#### 4.2.3 Direct Transmission

Under direct transmission, a source node does not perform CC and transmits directly to its destination node. The time-slot for each source node is  $t/N$ . For a session ( $s_i, d_i$ ), the achievable rate under direct transmission is

$$C_{\text{D}}(s_i, d_i) = \left( \frac{t}{N} \right) \cdot W \log_2(1 + \text{SNR}_{s_i d_i}) = \frac{W}{N} \cdot \log_2(1 + \text{SNR}_{s_i d_i}). \quad (23)$$

## 5 THE CASE OF DNC-CC

We now consider the digital version of NC-CC. We organize this section as follows. In Section 5.1, we give an upper bound and a lower bound on the rates at which source nodes can transmit data. In Section 5.2, we analyze DNC noise and the rate at which each destination node can receive. In Section 5.3, we derive the achievable rate for a session under DNC-CC.

### 5.1 Analyzing Transmission Rate at a Source Node

We first discuss the rate at which each source node can transmit data. We know that the relay node has to decode and then combine the signals transmitted by all the source nodes. However, the rates at which each source node can transmit varies. It is well known that in general, when multiple source nodes transmit data at different rates, the optimal DNC strategy remains unknown [3], [14], [26]. In addition to combining bits at the relay node, extraction and signal combination also need to be carried out at destination nodes. This makes designing an optimal procedure to perform DNC-CC even more complicated. So instead of trying to find an optimal DNC-CC strategy, we will present an upper bound and a lower bound for the transmission rate.

An upper bound for the transmission rate can be obtained by having every source node transmit at the maximum possible rate at which relay node can decode the data. This can be written as

$$I_{\text{DNC-CC}}^{\text{UB}}(s_i, r) = \log_2(1 + \text{SNR}_{s_i r}). \quad (24)$$

Equation (24) gives an upper bound on the transmission rate of  $s_i$  in bits/sec/Hz. This is because for any feasible (including optimal) scheme, a source node cannot transmit data at a rate that is greater than  $I_{\text{DNC-CC}}^{\text{UB}}(s_i, r)$ . Otherwise, the relay node will not be able to decode the signal as

required in the DF scheme. As a result, the transmission rate for source  $s_i$  under any feasible scheme cannot be greater than  $I_{\text{DNC-CC}}^{\text{UB}}(s_i, r)$ . It is important to note that a DNC strategy to combine the data streams remains unknown when every source node transmits at its maximum possible rate. So Eq. 24 will serve as an upper bound.

Further, any feasible DNC strategy will require each source node to transmit at some transmission rate (e.g., all source nodes transmit at the same rate). This transmission rate cannot be greater than the optimal transmission rate of that source node. As a result, a feasible DNC strategy will give us a lower bound on the rate at which each source node can transmit. One feasible strategy is to denote the source node that transmits at the lowest rate as the bottleneck source node; and to limit all the source nodes to transmit at this bottleneck rate. This will enable the relay node to perform bit by bit combination of the decoded data. A lower bound on the rate at which a source node  $s_i$  can transmit can be written as

$$I_{\text{DNC-CC}}^{\text{LB}}(s_i, r) = \log_2 \left( 1 + \min_{s_j \in \mathcal{S}_r} \{ \text{SNR}_{s_j r} \} \right). \quad (25)$$

## 5.2 Analyzing Reception Rate at a Destination Node

To study the reception rate at the destination nodes, we begin by analyzing the DNC noise. We first focus on the simple two-session network in Fig. 5(a). For this network, the signal transmitted by  $s_0$  and received by  $r$  in the first time slot is given by (1). Similarly, the signal transmitted by  $s_1$  and received by  $r$  in the second time slot is given by (3). The relay node  $r$  will decode the two signals, combine them using DNC, and then transmit the combined signal. The combined signal at  $r$  can be written as  $(x_0 + x_1)$ .

To understand the signal extraction process at a destination node, consider node  $d_1$ . The combined signal transmitted by  $r$  and received by node  $d_1$  can be written as

$$y_{rd_1}(t) = h_{rd_1} [x_0(t_1) + x_1(t_2)] + z_{d_1}(t), \quad \forall t \in (2T, 3T], \quad (26)$$

where  $x_0(t_1)$  is the signal transmitted by  $s_0$  in the first time slot, and  $x_1(t_2)$  is the signal transmitted by  $s_1$  in the second time slot. Note that when all source nodes are transmitting at the same rate (i.e., the lower bound case in Section 5.1),  $t_1 = t - 2T$  and  $t_2 = t - T$ . However, as the optimal NC strategy in general is unknown, we use general notation of  $t_1$  and  $t_2$ . We assume that the destination nodes know the values of  $t_1$  and  $t_2$  for any  $t$  (i.e., it knows the NC scheme that is employed by the relay node).

The destination node now has to subtract the  $x_0$  signal component from (26) in order to extract  $x_1$ . The signal for  $x_0$  overheard by  $d_1$  from  $s_0$  in the first time slot is given by (2). Assuming channel gains are known,  $d_1$  can extract the signal for  $x_1$  by multiplying (2) by  $\frac{h_{rd_1}}{h_{s_0d_1}}$  and

then subtract the product from (26).<sup>1</sup> The extracted signal can be written as

$$\begin{aligned} \bar{y}_{rd_1}(t) &= y_{rd_1}(t) - \frac{h_{rd_1}}{h_{s_0d_1}} y_{s_0d_1}(t_1) \\ &= h_{rd_1} x_1(t_2) + z_{d_1}(t) + \frac{h_{rd_1}}{h_{s_0d_1}} z_{d_1}(t_1), \\ &\quad \forall t \in (2T, 3T]. \end{aligned} \quad (27)$$

We can see that instead of  $z_{d_1}$ , we have a new noise term, which we call ‘‘DNC noise’’ and is denoted as  $z_{d_1}^{\text{DNC}}$ , i.e.,

$$z_{d_1}^{\text{DNC}} = z_{d_1}(t) + \frac{h_{rd_1}}{h_{s_0d_1}} z_{d_1}(t_1), \quad \forall t \in (2T, 3T]. \quad (28)$$

From (28), the variance of DNC noise is

$$\sigma_{z_{d_1}^{\text{DNC}}}^2 = \sigma_{d_1}^2 + \sigma_{d_1}^2 \left( \frac{h_{rd_1}}{h_{s_0d_1}} \right)^2. \quad (29)$$

For a general network with  $n$  sessions [i.e., Fig. 5(b)], where a group of source nodes in  $\mathcal{S}_r$  share the same relay node  $r$ , DNC noise at a destination node  $d_i$  can be obtained by generalizing (29). We have

$$\sigma_{z_{d_i}^{\text{DNC}}}^2 = \sigma_{d_i}^2 + \sigma_{d_i}^2 \sum_{s_j \in \mathcal{S}_r}^{j \neq i} \left( \frac{h_{rd_i}}{h_{s_j d_i}} \right)^2. \quad (30)$$

From (30), we can see that the variance of DNC noise increases monotonically as the number of sessions sharing the relay node.

By using the variance of DNC noise we can determine the rate at which a given destination node can receive its desired signal. Similar to the ANC-CC case, (17) and (27) can be written in a compact matrix form as

$$\mathbf{Y} = \mathbf{H}x_i + \mathbf{BZ}, \quad (31)$$

where

$$\mathbf{Y} = \begin{bmatrix} y_{s_i d_i} \\ \bar{y}_{rd_i} \end{bmatrix}, \quad \mathbf{H} = \begin{bmatrix} h_{s_i d_i} \\ h_{rd_i} \end{bmatrix},$$

$$\mathbf{B} = \begin{bmatrix} 1 & 0 \\ 0 & 1 \end{bmatrix}, \quad \text{and} \quad \mathbf{Z} = \begin{bmatrix} z_{d_i} \\ z_{d_i}^{\text{DNC}} \end{bmatrix}.$$

Similar to [16], we can model the above channel as a one-input two-output complex Gaussian vector channel. The rate at which destination node  $d_i$  can receive signal  $x_i$  is

$$I_{\text{DNC-CC}}(s_i \cup r, d_i) = \log_2 \det \left( \mathbf{I} + (\mathbf{P}\mathbf{H}\mathbf{H}^\dagger)(\mathbf{B}\mathbf{E}[\mathbf{Z}\mathbf{Z}^\dagger]\mathbf{B}^\dagger)^{-1} \right),$$

where

$$\mathbf{E}[\mathbf{Z}\mathbf{Z}^\dagger] = \begin{bmatrix} \sigma_{d_i}^2 & 0 \\ 0 & \sigma_{z_{d_i}^{\text{DNC}}}^2 \end{bmatrix}, \quad \text{and} \quad \mathbf{P} = \begin{bmatrix} P_{s_i} & 0 \\ 0 & P_r \end{bmatrix}.$$

1. Another possible approach to perform signal extraction is for  $d_1$  to first decode  $y_{s_0d_1}$  and then use the extracted  $x_0$  to perform a subtraction. However, such an approach places excessive restriction on the rate at which source nodes can transmit their signals, and is likely to perform worse than the approach we use here.

Expanding (32) gives us

$$I_{\text{DNC-CC}}(s_i \cup r, d_i) = \log_2 \left( 1 + \frac{P_{s_i} |h_{s_i d_i}|^2}{\sigma_{d_i}^2} + \frac{P_r |h_{r d_i}|^2}{\sigma_{z_{d_i}^{\text{DNC}}}^2} \right),$$

which can be further rewritten as

$$I_{\text{DNC-CC}}(s_i \cup r, d_i) = \log_2 \left( 1 + \text{SNR}_{s_i d_i} + \frac{\text{SNR}_{r d_i}}{\frac{\sigma_{z_{d_i}^{\text{DNC}}}^2}{\sigma_{d_i}^2}} \right). \quad (32)$$

From (32), we can see that the rate at which destination nodes can receive data decreases when the variance of DNC noise increases.

We now have the rate for each source node to transmit [i.e., either (24) or (25)] and the rate for each destination node to receive [i.e., (32)]. For any given session, the minimum of the source transmission rate and the destination reception rate is the achievable rate for that session. As a result, the minimum of (24) and (32) gives us an upper bound for the mutual information for session  $(s_i, d_i)$ . Similarly, the minimum of (25) and (32) gives us a lower bound for the mutual information for a session  $(s_i, d_i)$  under DNC-CC.

### 5.3 Computing Achievable Rate

Similar to the analog case, we assume that each frame has a length of  $t$  (seconds) and each time slot in the frame has a length of  $T$ . Then,  $T = \frac{t}{N+1}$ . Under such setting, we can write the upper bound on the achievable rate of  $(s_i, d_i)$  for DNC-CC as

$$C_{\text{DNC-CC}}^{\text{UB}}(s_i, r, d_i) = \frac{W}{N+1} \cdot \min \{ I_{\text{DNC-CC}}^{\text{UB}}(s_i, r), I_{\text{DNC-CC}}(s_i \cup r, d_i) \}, \quad (33)$$

and the lower bound on the achievable rate of  $(s_i, d_i)$  as

$$C_{\text{DNC-CC}}^{\text{LB}}(s_i, r, d_i) = \frac{W}{N+1} \cdot \min \{ I_{\text{DNC-CC}}^{\text{LB}}(s_i, r), I_{\text{DNC-CC}}(s_i \cup r, d_i) \}. \quad (34)$$

Note that when  $|\mathcal{S}_r| = 1$ , i.e., one-session (three-node model), we have  $\sigma_{z_{d_i}^{\text{DNC}}}^2 = \sigma_{d_i}^2$ , and both (33) (upper bound) and (34) (lower bound) reduce to

$$C_{\text{DF}}(s_i, r, d_i) = \frac{W}{2} \min \left\{ \log_2 (1 + \text{SNR}_{s_i r}), \log_2 (1 + \text{SNR}_{s_i d_i} + \text{SNR}_{r d_i}) \right\},$$

which is exactly the result for the three-node model given in [16].

**DF CC (without DNC).** It is worth comparing the achievable rate under DNC-CC with DF CC when DNC is not used. Under the latter scheme, every source node

and the relay node gets equal time slot duration of  $\frac{t}{2N}$ . The achievable rate of a session  $(s_i, d_i)$  is [16]:

$$C_{\text{DF}}(s_i, r, d_i) = \frac{W}{2N} \min \left\{ \log_2 \left( 1 + \frac{|h_{s_i r}|^2 P_{s_i}}{\sigma_r^2} \right), \log_2 \left( 1 + \frac{|h_{r d_i}|^2 P_r}{\sigma_{d_i}^2} + \frac{|h_{s_i d_i}|^2 P_{s_i}}{\sigma_{d_i}^2} \right) \right\}. \quad (35)$$

## 6 NUMERICAL RESULTS

In this section, we present some numerical results to show the impact of NC on CC, in the light of NC noise. We assume that the total bandwidth in the network  $W = 22$  MHz [10]. All source nodes transmit with 1 W of power. The variance of Gaussian noise at each node is  $10^{-10}$  W, and the path loss index is 4. For simplicity, the channel gain  $|h_{uv}|^2$  between two nodes is modeled as  $d_{uv}^{-4}$ , where  $d_{uv}$  is the distance between  $u$  and  $v$ , and 4 is the path loss index.

The results are divided into two parts. In the first part, we use simple two-session networks to illustrate that NC can be either a friend or a foe of CC, depending on network settings. So a blind use of NC in CC is not advisable. The second part consists of a general network with multiple sessions. Here, we quantify the impact of DNC noise and ANC noise on the achievable rate of individual sessions. Our results show that as the number of sessions that share the same relay node increases, the benefit of NC in CC diminishes, gradually switching NC from a friend to a foe.

### 6.1 Two-Session Networks

#### 6.1.1 NC as a Friend

We first show that in certain network settings, NC-CC can offer better data transmission rates than CC or direct transmission schemes. A network topology illustrating this case is shown in Fig. 8.

**The Analog Case (ANC-CC).** For ANC-CC, the results are shown in Table 2 and Fig. 9. There are four columns in Table 2. The first column shows the source and destination nodes of each session. The second column shows the achievable rates under ANC-CC [i.e. based on Eq. (15)]. The third column shows the achievable rate for each session when the session performs AF CC without the use of ANC [i.e., based on Eq. (22)]. The last column shows the achievable rate of the sessions under direct transmission [i.e. based on Eq. (23)].

We can see that for the topology in Fig. 8, the achievable rates under ANC-CC are higher than the achievable rates under AF CC without ANC, as well as the rates under direct transmission. Figure 9 shows the results for the outage probability of session  $(s_0, d_0)$  under ANC-CC, AF CC, and direct transmission schemes. The results for session  $(s_1, d_1)$  are similar and are thus omitted. For each scheme, the outage probability is computed by counting the number of outages under 10,000 channel realizations. We assume that all channels in the network are Rayleigh faded. Figure 9 shows that the outage probability of session  $(s_0, d_0)$  under

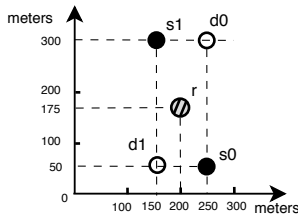


Fig. 8. A network topology where NC is a friend of CC.

TABLE 2

Comparison of achievable rates when ANC is a friend.

Session	ANC-CC (Mb/s)	AF CC (Mb/s)	Direct Transmission (Mb/s)
$(s_0, d_0)$	23.75	22.09	19.22
$(s_1, d_1)$	23.75	22.09	19.22

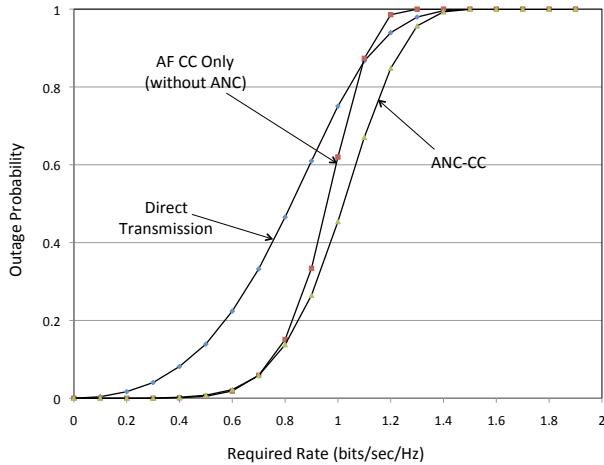


Fig. 9. Outage probabilities of session  $(s_0, d_0)$  when ANC is a friend.

ANC-CC is lower than that under AF CC scheme and direct transmission.

**The Digital Case (DNC-CC).** For DNC-CC, the results are shown in Table 3 and Fig. 10. The columns in Table 3 are similar to those in Table 2, except that the achievable rate under DNC-CC is represented by an upper bound and a lower bound in the second and third columns. By noting that the upper and lower bounds for both sessions are identical, we conclude that the rates in columns 2 and 3 are the optimal rates. We can see that the achievable rates under DNC-CC (columns 2 and 3) are better than those under DF CC without DNC (column 4), as well as the rate under direct transmission (i.e., the last column in Table 3). Further, Fig. 10 shows that the outage probabilities of session  $(s_0, d_0)$  under DNC-CC are also lower than those under DF CC and direct transmission.

Note that the above results for ANC-CC and DNC-CC can also be explained intuitively. To extract the desired signal from the combined signal, node  $d_0$  has to subtract the overheard signal from  $s_1$ . From Fig. 8, we see that since  $s_1$  is closer to  $d_0$ , this gives  $d_0$  a better reception of the signal from  $s_1$ . As a result, the NC noise component in the extracted signal at  $d_0$  is small, which makes NC a friend of CC. Similar discussion also holds for session  $(s_1, d_1)$  in

TABLE 3

Comparison of achievable rates when DNC is a friend.

Session	DNC-CC (Mb/s)		DF CC (Mb/s)	Direct Transmission (Mb/s)
	LB	UB		
$(s_0, d_0)$	33.22	33.22	26.09	19.22
$(s_1, d_1)$	33.22	33.22	26.09	19.22

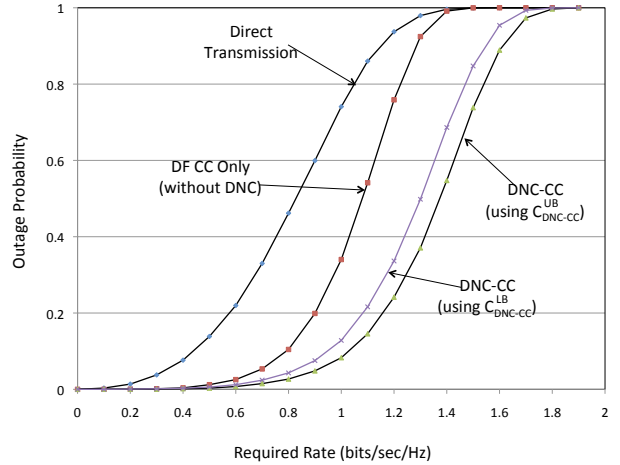


Fig. 10. Outage probabilities of session  $(s_0, d_0)$  when DNC is a friend.

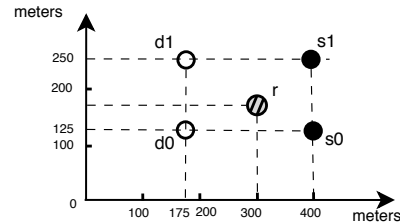


Fig. 11. A network topology where NC is a foe of CC.

Fig. 8.

### 6.1.2 NC as a Foe

We now show that NC may not always benefit CC. A network topology illustrating this case is shown in Fig. 11.

**The Analog Case (ANC-CC).** For ANC-CC, the results are shown in Table 4 and Fig. 12. Table 4 shows that for both sessions, the achievable rates under ANC-CC (column 2) are lower than those under AF CC and direct transmission, respectively. Figure 12 shows that over a wide range, the outage probabilities of session  $(s_0, d_0)$  under ANC-CC are higher than those under AF CC and direct transmission.

**The Digital Case (DNC-CC).** Similar to the analog case, Table 5 shows that for both sessions, the achievable rates under DNC-CC (column 2 and 3) are lower than those under DF CC and direct transmission, respectively. Figure 13 shows that over a wide range, the outage probabilities of session  $(s_0, d_0)$  under DNC-CC are higher than those under DF CC and direct transmission. Note that in Fig. 13, the plots for the lower and upper bounds on the outage probability under the DNC-CC scheme overlap with each other.

Note that the above results for ANC-CC and DNC-CC

TABLE 4  
Comparison of achievable rates when ANC is a foe.

Session	ANC-CC (Mb/s)	AF CC (Mb/s)	Direct Transmission (Mb/s)
$(s_0, d_0)$	20.50	24.45	24.06
$(s_1, d_1)$	18.20	22.30	24.06

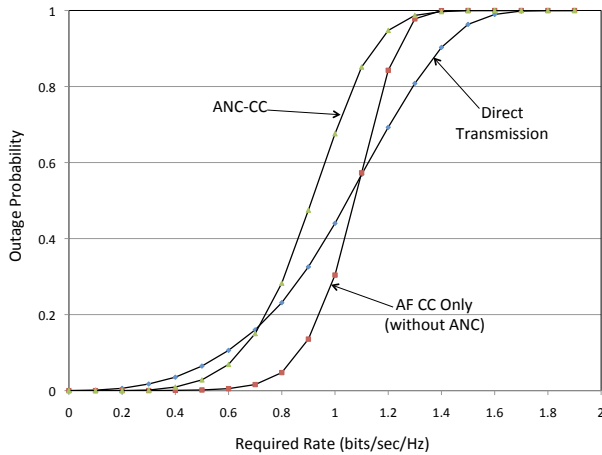


Fig. 12. Outage probabilities of session  $(s_0, d_0)$  when ANC is a foe.

TABLE 5  
Comparison of achievable rate when DNC is a foe.

Session	DNC-CC (Mb/s)		DF CC (Mb/s)	Direct Transmission (Mb/s)
	LB	UB		
$(s_0, d_0)$	19.66	19.66	26.98	24.06
$(s_1, d_1)$	19.59	19.59	24.95	24.06

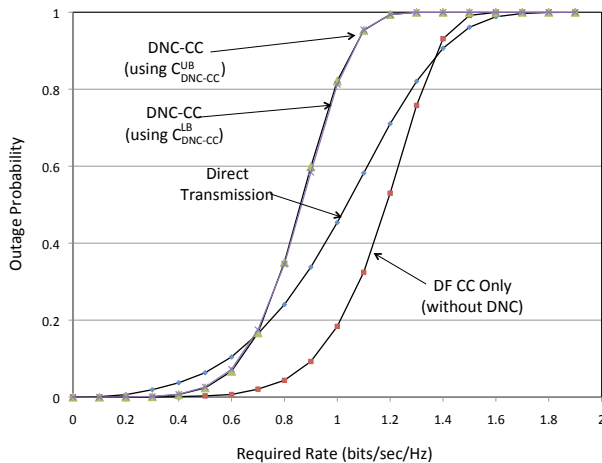


Fig. 13. Outage probabilities of session  $(s_0, d_0)$  when DNC is a foe.

can also be explained intuitively. To extract the desired signal from the combined signal, node  $d_0$  has to subtract the signal overheard from  $s_1$ . From Fig. 11, we see that source  $s_1$  is far away from  $d_0$ . This results in weaker reception of  $s_1$ 's signal at  $d_0$ . Therefore, the NC noise component in the extracted signal at  $d_0$  is high, which makes NC a foe of CC. Similar discussion also holds for session  $(s_1, d_1)$  in Fig. 11. However, we can see that the effect of NC noise on  $(s_1, d_1)$  is more than that on  $(s_0, d_0)$ . This can be explained by observing that node  $d_1$  is farther away from  $r$  as compared

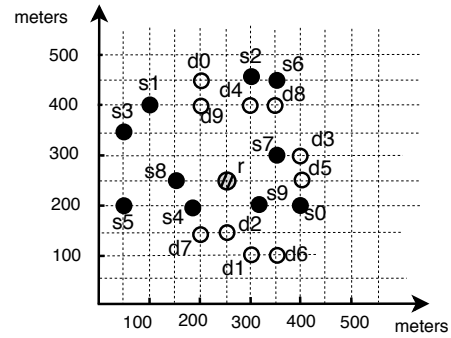


Fig. 14. A 10-session one-relay network topology.

to node  $d_0$ , resulting in comparatively weaker reception of network coded signal at  $d_1$ .

### 6.1.3 Summary

The above two scenarios illustrate that NC can be either a friend or a foe of CC. That is, the NC noise infused at the destination nodes could undermine the time slot advantage of NC-CC. When NC noise is sufficiently large, the advantage of NC-CC diminishes and NC becomes a foe of CC.

## 6.2 A General Multi-Session Network

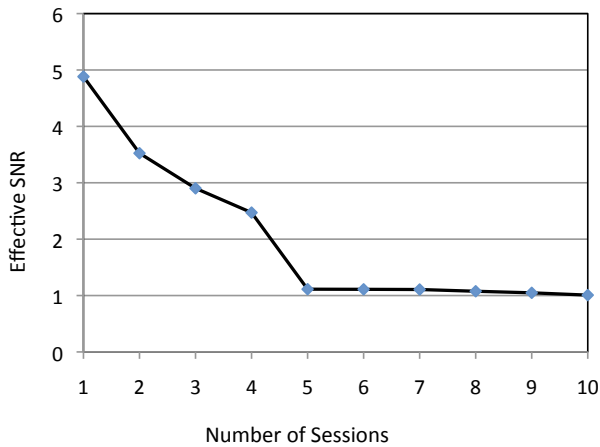
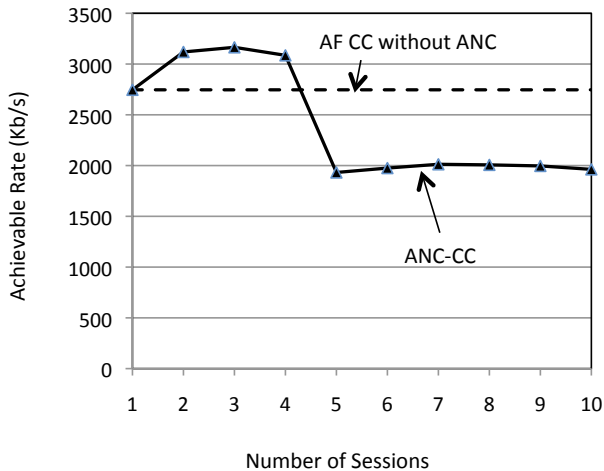
In this section, we consider a general network with multiple sessions. The network topology is shown in Fig. 14, where we have 10 sessions and one relay node. We show that when more sessions employ NC-CC and share the same relay node, NC noise at destination nodes will increase. This increase in NC noise will have a direct impact on the effective SNR and the achievable rate of individual sessions. As a result, when the amount of NC noise increases beyond a certain threshold, NC will switch from a friend to a foe of CC. We chose session  $(s_0, d_0)$  in our study to demonstrate these findings under both ANC-CC and DNC-CC.

**The Analog Case (ANC-CC).** To start with, all the sessions are active, but only one session  $(s_0, d_0)$  is using the relay node  $r$  to perform AF CC. The effective bandwidth for each session is  $W/10$ . We first determine the effect of adding more sessions on the effective SNR of  $(s_0, d_0)$ . Here, the effective SNR for a session  $(s_i, d_i)$  is defined based on (15), i.e.,

$$\text{SNR}_{\text{eff}}^{\text{ANC}}(s_i, r, d_i) = \text{SNR}_{s_i d_i} + \frac{\text{SNR}_{s_i r} \text{SNR}_{r d_i}}{\left| \mathcal{S}_r \right| \frac{\sigma_{z_{d_i}}^{\text{new}}}{\sigma_{d_i}^2} + \text{SNR}_{r d_i} + \frac{\sigma_{z_{d_i}}^{\text{new}}}{\sigma_{d_i}^2} \sum_{s_j \in \mathcal{S}_r} \text{SNR}_{s_j r}}}, \quad (36)$$

where  $\mathcal{S}_r$  is the set for those source nodes using relay node  $r$ .

Since only one session [i.e.,  $(s_0, d_0)$ ] is using the relay node initially, the value of  $N(= |\mathcal{S}_r|)$  in Eq. (36) will be one for session  $(s_0, d_0)$ , and  $\mathcal{S}_r$  will contain only  $s_0$ . Then we let session  $(s_1, d_1)$  also share the relay node. Now both  $(s_0, d_0)$  and  $(s_1, d_1)$  are employing ANC-CC, and the other

(a) Impact on effective SNR for session  $(s_0, d_0)$ .(b) Impact on achievable rate for session  $(s_0, d_0)$ .Fig. 15. The impact on session  $(s_0, d_0)$  as more sessions share the same relay node.

eight sessions are using direct transmission. Note that now, the value of  $N(=|\mathcal{S}_r|)$  in (36) for these two sessions will be two, and  $\mathcal{S}_r$  will contain  $\{s_0, s_1\}$ . The process continues until all 10 sessions share the same relay node.

We plot the effective SNR of session  $(s_0, d_0)$  as more sessions are using the same relay in Fig. 15(a). We can see that as more sessions start using the relay node, the effective SNR of session  $(s_0, d_0)$  decreases. This is due to the increase in the ANC noise at the destination node for session  $(s_0, d_0)$ .

This reduction in the effective SNR of session  $(s_0, d_0)$  affects the achievable rate of this session. This impact is illustrated in Fig. 15(b). We plot two curves in Fig. 15(b). The solid curve shows the achievable rate of session  $(s_0, d_0)$ , which is calculated using (15). The straight dotted line shows the achievable rate of session  $(s_0, d_0)$  when ANC is not used [i.e., Eq. (22)]. In Fig. 15(b), we find that NC remains a friend of CC for session  $(s_0, d_0)$  initially due

TABLE 6  
Comparison of various data communication schemes with ANC-CC for a 10-session network.

Session	ANC-CC (Mb/s)	AF CC (Mb/s)	Direct Transmission (Mb/s)
$(s_0, d_0)$	1.92	2.68	2.02
$(s_1, d_1)$	1.36	2.49	1.41
$(s_2, d_2)$	2.00	2.70	2.05
$(s_3, d_3)$	1.40	2.34	1.50
$(s_4, d_4)$	4.81	4.43	4.37
$(s_5, d_5)$	0.92	2.13	0.97
$(s_6, d_6)$	1.44	2.20	1.55
$(s_7, d_7)$	5.53	5.49	5.39
$(s_8, d_8)$	3.89	3.78	3.84
$(s_9, d_9)$	4.86	4.43	4.37

to the time-slot benefit of NC. However, as more sessions start sharing the same relay node, the adverse effect of ANC noise at  $d_0$  starts to increase, and the achievable rate of session  $(s_0, d_0)$  starts to decrease. Finally, when five sessions share the relay node, the ANC noise reaches a point where the time-slot benefit of ANC-CC is no longer able to offset the adverse effect of ANC noise. At this point, NC switches from a friend to a foe of CC.

We now consider the final instance when all the sessions in the network are using the same relay node to perform ANC-CC. Table 6 shows the achievable rates of all the sessions in the network under different transmission schemes (similar to Tables 2 and 4). As one can see, there is no definitive statement on which scheme is better, when considering all 10 sessions jointly.

**The Digital Case (DNC-CC).** Following the same process as in the analog case, we let multiple sessions share the same relay node. Initially, only one session  $(s_0, d_0)$  is using the relay node  $r$  to perform DF CC. Afterwards, other sessions start sharing the relay node one by one. The process continues until all 10 sessions share the same relay node.

Similar to the analog case, Fig. 16(b) shows that the reduction in effective SNR directly impacts the achievable rate of  $(s_0, d_0)$  in DNC-CC. We can see that the achievable rate for session  $(s_0, d_0)$  under DNC-CC falls below the achievable rate under DF CC when five or more sessions share the relay node. This is the point where NC switches from a friend to a foe.

Table 7 shows the achievable rates when all 10 sessions in the network share the same relay node under DNC-CC (similar to Table 6 for the analog case). We observe that the achievable rate under DNC-CC is lower than that under the DF CC scheme for all the sessions. This shows that by having all the sessions share the same relay node, the benefit of NC in CC diminishes.

Figure 16(a) shows the effect of adding more sessions on the effective SNR of session  $(s_0, d_0)$ . The lower and the upper bounds on the effective SNR under DNC-CC are

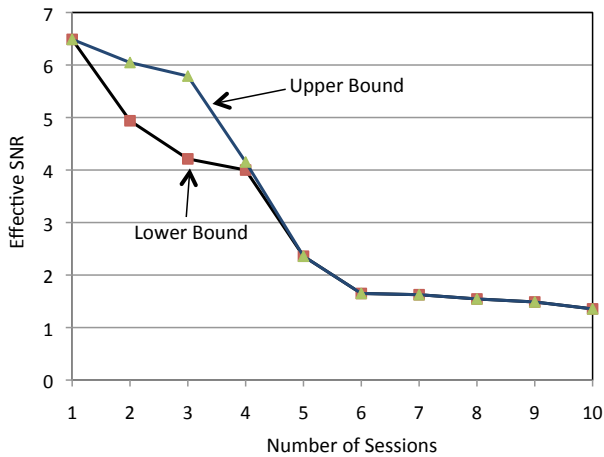
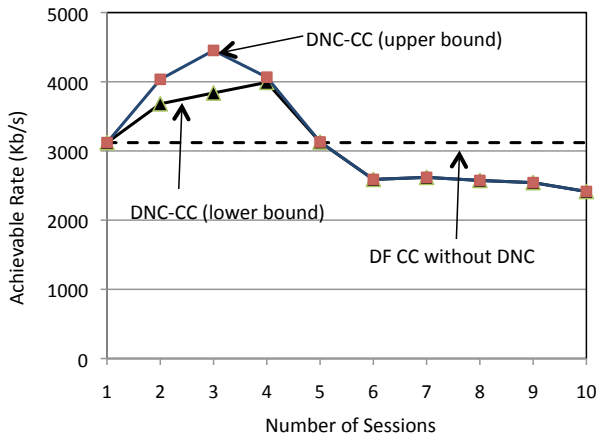
(a) Impact on effective SNR for session  $(s_0, d_0)$ .(b) Impact on achievable rate for session  $(s_0, d_0)$ .Fig. 16. The impact on session  $(s_0, d_0)$  as more sessions share the same relay node.

TABLE 7

Comparison of various data communication schemes with DNC-CC for a 10-session network.

Session	DNC-CC (Mb/s)		DF CC (Mb/s)	Direct Transmission (Mb/s)
	LB	UB		
$(s_0, d_0)$	2.36	2.36	3.05	2.02
$(s_1, d_1)$	1.55	1.55	2.70	1.41
$(s_2, d_2)$	2.32	2.32	2.50	2.05
$(s_3, d_3)$	1.77	1.77	2.44	1.50
$(s_4, d_4)$	4.24	4.24	4.55	4.37
$(s_5, d_5)$	1.14	1.14	2.84	0.97
$(s_6, d_6)$	1.60	1.60	2.44	1.55
$(s_7, d_7)$	4.43	5.02	6.32	5.39
$(s_8, d_8)$	3.69	3.69	3.89	3.84
$(s_9, d_9)$	4.35	4.35	4.55	4.37

defined based on (33) and (34), and are written as

$$\text{SNR}_{\text{eff-DNC}}^{\text{LB}}(s_i, r, d_i) = \min \left\{ \min_{s_j \in \mathcal{S}_r} \{ \text{SNR}_{s_j r} \}, \left( \text{SNR}_{s_i d_i} + \frac{\text{SNR}_r d_i}{\frac{\sigma_z^2 \text{DNC}}{\sigma_{d_i}^2}} \right) \right\},$$

$$\text{SNR}_{\text{eff-DNC}}^{\text{UB}}(s_i, r, d_i) =$$

$$\min \left\{ \text{SNR}_{s_j r}, \left( \text{SNR}_{s_i d_i} + \frac{\text{SNR}_r d_i}{\frac{\sigma_z^2 \text{DNC}}{\sigma_{d_i}^2}} \right) \right\}.$$

We can see that after four sessions, the plot for the lower bound and upper bound coincides with each other.

**Summary.** From the above results, we find that NC can benefit CC only when the number of sessions sharing the same relay node is small. As such number increases, NC noise also increases (both in the analog case or the digital case), and the benefit of NC in CC diminishes. Note that the quantitative effect of ANC on AF-CC is different from that of DNC on DF-CC. This is due to the physical difference between the two schemes. A quantitative comparison between the two schemes is beyond the scope of this paper.

## 7 CONCLUSION

In this paper, we investigated the fundamental problem of how NC can affect the performance of CC. In contrary to current perception, NC can be both a friend or a foe of CC, depending on the underlying network setting. The reason for such uncertainty is the existence of NC noise, which is the key factor that hinders the performance of NC-CC. In this paper, we formalized the concept of NC noise and characterized it mathematically both for the analog case (ANC-CC) and digital case (DNC-CC). We also derived mutual information and achievable rate calculations under ANC-CC and DNC-CC. Using numerical results, we demonstrated the impact of NC on CC. Our results offer new understanding on NC-CC and provide guidelines on its future application in practice.

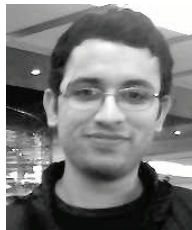
Our findings in this paper lay the foundation for the design of MAC and network layer protocols for NC-CC. Here, we briefly discuss some important problems that we envision for MAC/network layer protocol design. We start with the simple problem where there are multiple sessions and only one relay node. For a given objective, a MAC problem could be how to group sessions and assign time slot for each session. Note that the problem is further complicated by the fact that some sessions may be better-off by using direct transmission instead of NC-CC. In the case when multiple relay nodes are present, the problem becomes much harder. At the network layer, when data transport between a source and its destination node requires multiple hops, we need to consider how to assign an available node for physical layer relay (NC-CC) or network layer relay (i.e., the multihop relay). The solutions to these problems remain open and should be explored as future work.

## ACKNOWLEDGMENTS

The work of Y.T. Hou, S.F. Midkiff, S. Sharma, and Y. Shi has been supported in part by the NSF under Grant CNS-1064953. The work of S. Kompella has been supported in part by the ONR.

## REFERENCES

- [1] R. Ahlswede, N. Cai, S.-Y.R. Li, and R.W. Yeung, "Network information flow," *IEEE Transactions on Information Theory*, vol. 46, issue 4, pp. 1204–1216, July 2000.
- [2] X. Bao, and J. Li, "Adaptive network coded cooperation (ANCC) for wireless relay networks: matching code-on-graph with network-on-graph," *IEEE Transactions on Wireless Communications*, vol. 7, no. 2, pp. 574–583, February 2008.
- [3] M. Chen, M. Ponec, S. Sengupta, J. Li, and P.A. Chou, "Utility maximization in peer-to-peer systems," In *Proceedings of ACM SIGMETRICS*, pp. 169–180, Annapolis, Maryland, June 2–6, 2008.
- [4] T.M. Cover and A. EL Gamal, "Capacity theorems for the relay channel," *IEEE Transactions on Information Theory*, vol. 25, issue 5, pp. 572–584, September 1979.
- [5] M.O. Damen and A.R. Hammons, "Delay-tolerant distributed-TAST codes for cooperative diversity," *IEEE Transactions on Information Theory*, vol. 53, no. 10, pp. 3755–3773, Oct. 2007.
- [6] D. Gunduz and E. Erkip, "Opportunistic cooperation by dynamic resource allocation," *IEEE Transactions on Wireless Communications*, vol. 6, no. 4, pp. 1446–1454, April 2007.
- [7] O. Gurewitz, A. de Baynast, and E.W. Knightly, "Cooperative strategies and achievable rate for tree networks with optimal spatial reuse," *IEEE Transactions on Information Theory*, vol. 53, no. 10, pp. 3596–3614, Oct. 2007.
- [8] The network coding home page: <http://www.ifp.uiuc.edu/koetter/NWC/index.html>
- [9] T.E. Hunter and A. Nosratinia, "Diversity through coded cooperation," *IEEE Transactions on Wireless Communications*, vol. 5, no. 2, pp. 283–289, February 2006.
- [10] IEEE 802.11: Wireless LAN medium access control (MAC) and physical layer (PHY) specifications: <http://standards.ieee.org/getieee802/download/802.11-2007.pdf>
- [11] S. Katti, H. Rahul, W. Hu, D. Katabi, M. Medard, and J. Crowcroft, "XORs in the air: practical wireless network coding," In *Proceedings of ACM SIGCOMM*, pp. 497–510, Pisa, Italy, September 11–15, 2006.
- [12] S. Katti, S. Gollakotta, and D. Katabi, "Embracing wireless interference: analog network coding," In *Proceedings of ACM SIGCOMM*, pp. 397–408, Kyoto, Japan, August 27–31, 2007.
- [13] A.E. Khandani, J. Abounadi, E. Modiano, and L. Zheng, "Cooperative routing in static wireless networks," *IEEE Transactions on Communications*, vol. 55, no. 11, pp. 2185–2192, Nov. 2007.
- [14] M. Kim, M. Medard, U-M. O'Reilly, and D. Traskov, "An evolutionary approach to inter-session network coding," In *Proceedings of IEEE INFOCOM*, pp. 450–458, Rio de Janeiro, Brazil, April 19–25, 2009.
- [15] G. Kramer, I. Maric, and R.D. Yates, "Cooperative communications," *Foundations and Trends in Networking*, Now Publishers, June 2007.
- [16] J.N. Laneman, D.N.C. Tse, and G.W. Wornell, "Cooperative diversity in wireless networks: efficient protocols and outage behavior," *IEEE Transactions on Information Theory*, vol. 50, no. 12, pp. 3062–3080, Dec. 2004.
- [17] C. Peng, Q. Zhang, M. Zhao, and Y. Yao, "On the performance analysis of network-coded cooperation in wireless networks," In *Proceedings of IEEE INFOCOM*, pp. 1460–1468, Anchorage, Alaska, May 6–12, 2007.
- [18] S. Savazzi, and U. Spagnolini, "Energy aware power allocation strategies for multihop-cooperative transmission schemes," *IEEE Journal on Selected Areas in Communications*, vol. 25, no. 2, pp. 318–327, February 2007.
- [19] Y.E. Sagduyu, D. Guo, and R. Berry, "On the delay and throughput of digital and analog network coding for wireless broadcast," In *Proceedings of 44<sup>th</sup> Annual Conference on Information Sciences and Systems*, pp. 534–539, Princeton, NJ, March 19–21, 2008.
- [20] A. Scaglione, D.L. Goeckel, and J.N. Laneman, "Cooperative communications in mobile ad hoc networks," *IEEE Signal Processing Magazine*, vol. 23, no. 5, pp. 18–29, Sept. 2006.
- [21] A. Sendonaris, E. Erkip, and B. Aazhang, "User cooperation diversity – part I: system description," *IEEE Transactions on Communications*, vol. 51, no. 11, pp. 1927–1938, Nov. 2003.
- [22] A. Sendonaris, E. Erkip, and B. Aazhang, "User cooperation diversity – part II: implementation aspects and performance analysis," *IEEE Transactions on Communications*, vol. 51, no. 11, pp. 1939–1948, Nov. 2003.
- [23] E.C. van der Meulen, "Three terminal communication channels," *Advances in Applied Probability*, vol. 3, pp. 120–154, 1971.
- [24] L. Xiao, T.E. Fuja, J. Kliewer, and D.J. Costello, "A network coding approach to cooperative diversity," *IEEE Transactions on Information Theory*, vol. 53, no. 10, pp. 3714–3722, Oct. 2007.
- [25] H. Xu and B. Li, "XOR-assisted cooperative diversity in OFDMA wireless networks: optimization framework and approximation algorithms," In *Proceedings of IEEE INFOCOM*, pp. 2141–2149, Rio de Janeiro, Brazil, April 19–25, 2009.
- [26] X. Yan, R.Y. Yeung, and Z. Zhang, "The capacity region for multi-source multi-sink network coding," In *Proceedings of IEEE Symposium on Information Theory*, pp. 116–120, Nice, France, June 24–29, 2007.
- [27] E.M. Yeh and R.A. Berry, "Throughput optimal control of cooperative relay networks," *IEEE Transactions on Information Theory*, vol. 53, no. 10, pp. 3827–3833, Oct. 2007.



**Sushant Sharma** (S'06–M'11) received his B.E. degree in computer engineering from the University of Pune, India, in 2002, the M.S. degree in computer science from the University of New Mexico, Albuquerque, in 2005, and the Ph.D. degree in computer science from Virginia Tech, Blacksburg, VA, in 2010. He is currently working as a Research Associate in the Computational Science Center at Brookhaven National Laboratory, Upton, NY. His research interests

include developing novel algorithms to solve optimization problems in wired and wireless networks.



**Yi Shi** (S'02–M'08) received his B.S. degree from the University of Science and Technology of China, Hefei, China, in 1998, a M.S. degree from Institute of Software, Chinese Academy of Science, Beijing, China, in 2001, a second M.S. degree from Virginia Polytechnic Institute and State University ("Virginia Tech"), Blacksburg, VA, in 2003, all in computer science, and a Ph.D. degree in computer engineering from Virginia Tech, in 2007. He is currently a Research Scientist in

the Department of Electrical and Computer Engineering at Virginia Tech. Dr. Shi's research focuses on algorithms and optimization for cognitive radio networks, MIMO and cooperative communication networks, sensor networks, and ad hoc networks. He was a recipient of IEEE INFOCOM 2008 Best Paper Award. He was a recipient of Chinese Government Award for Outstanding Ph.D. Students Abroad in 2006. He served as a TPC member for many major international conferences (including ACM MobiHoc 2009 and IEEE INFOCOM 2009–2012).



**Jia Liu** (S'03–M'10) received his dual B.S. degrees in Electrical Engineering and Computer Science from South China University of Technology in 1996. He received his M.S. degree in Electrical Engineering from South China University of Technology in 1999. He received his Ph.D. degree in Electrical and Computer Engineering from Virginia Polytechnic Institute and State University (Virginia Tech) in 2010. From 1999–2003, Liu was a member of technical staff at Bell Labs, Lucent Technologies in Beijing, China. In April 2010, he joined Ohio State University as a Postdoctoral Research Scientist.

Liu's research focuses on MIMO technologies, multi-carrier communications systems, cognitive radio, information theory, and mathematical optimization theory for communications networks. His work has appeared in some highly selective international conferences (ACM MobiHoc and IEEE INFOCOM) and leading IEEE journals.

Liu is a member of IEEE and SIAM. He is a regular reviewer for major IEEE conferences and journals. He is a member of Tau Beta Pi. He was a recipient of Bell Labs President Gold Award in 2001. He was a recipient of IEEE ICC 2008 Best Paper Award. He was a recipient of Chinese Government Award for Outstanding Ph.D. Students Abroad in 2008. His paper was also the only Runner-up paper of IEEE INFOCOM 2011 Best Paper Award.



**Y. Thomas Hou** (S'91–M'98–SM'04) received his Ph.D. degree in Electrical Engineering from Polytechnic Institute of New York University in 1998. From 1997 to 2002, Dr. Hou was a Researcher at Fujitsu Laboratories of America, Sunnyvale, CA. Since 2002, he has been with Virginia Polytechnic Institute and State University ("Virginia Tech"), the Bradley Department of Electrical and Computer Engineering, Blacksburg, VA, where he is now an Associate Professor.

Prof. Hou's research interests are cross-layer design and optimization for cognitive radio wireless networks, cooperative communications, MIMO-based ad hoc networks, and new interference management schemes for wireless networks. He was a recipient of an Office of Naval Research (ONR) Young Investigator Award (2003) and a National Science Foundation (NSF) CAREER Award (2004) for his research on optimizations and algorithm design for wireless ad hoc and sensor networks.

Prof. Hou is currently serving as an Area Editor of *IEEE Transactions on Wireless Communications*, an Editor for *IEEE Transactions on Mobile Computing*, *IEEE Wireless Communications*, *ACM/Springer Wireless Networks (WINET)*, and *Elsevier Ad Hoc Networks*. He was a past Associate Editor of *IEEE Transactions on Vehicular Technology*. He was Technical Program Co-Chair of IEEE INFOCOM 2009.

Prof. Hou recently co-edited a textbook titled *Cognitive Radio Communications and Networks: Principles and Practices*, which was published by Academic Press/Elsevier, 2010.



**Sastry Kompella** (S'04–M'07) received the Ph.D. degree in electrical and computer engineering from Virginia Polytechnic Institute and State University, Blacksburg, VA, in 2006. Currently, he is a Researcher in the Information Technology Division, U.S. Naval Research Laboratory, Washington, DC. His research focuses on complex problems in cross-layer optimization and scheduling in wireless networks.



**Scott F. Midkiff** (S'82–M'85–SM'92) is Professor and Department Head in the Bradley Department of Electrical and Computer Engineering, Virginia Polytechnic Institute and State University, Blacksburg, VA. He received the B.S.E. and Ph.D. degrees from Duke University, Durham, NC, and the M.S. degree from Stanford University, Stanford, CA, all in Electrical Engineering. He worked at Bell Laboratories and held a visiting position at Carnegie Mellon University, Pittsburgh, PA.

He joined Virginia Tech in 1986. During 2006–2009, he served as a Program Director at the National Science Foundation. Dr. Midkiff's research and teaching interests include wireless and ad hoc networks, network services for pervasive computing, and cyber-physical systems.